Civil Engineering and Applied Solutions

Research Article

journal homepage: ceas.journals.umz.ac.ir

CEAS Civil Engineering and Applied Solutions

Effect of Subsurface Cavities on the Bearing Capacity of Shallow Strip Foundations in Soft Clay: A Numerical Study

Vali Ghaseminejad [a*], Atina Tarrah [a], Fereshteh Ghomi [a]

[a] *Department of Civil Engineering, Nowshahr Branch, Islamic Azad University, Nowshahr, Iran*

ARTICLE INFO

Keywords:
Shallow foundations
Bearing capacity
Subsurface cavities
Clay soils
Finite element analysis

Article history:
Received 19 August 2025
Accepted 22 October 2025
Available online 01 February 2026

ABSTRACT

Subsurface cavities, both natural and anthropogenic, pose significant geotechnical challenges by altering stress distribution beneath shallow foundations. Conventional design approaches for strip footings often neglect the effects of such voids, potentially resulting in unsafe or overly conservative designs. This study employs a numerical investigation using the finite element software PLAXIS 2D to assess the impact of underground cavities on the bearing capacity of shallow strip foundations resting on soft clay. A parametric analysis was conducted to examine the effects of cavity diameter, embedment depth, and both horizontal and vertical offsets relative to the footing center. The Results indicate that increasing cavity diameter markedly reduces the ultimate bearing capacity. Additionally, increasing the cavity diameter from 0.25 to 0.5 times the footing width led to a 25%–40% decrease in load-bearing capacity. The study also identifies a critical influence zone beneath the footing where the presence of voids most significantly compromises performance. These findings underscore the importance of incorporating subsurface cavity effects into geotechnical design, particularly in urban areas, to enhance the safety and reliability of shallow foundations on soft clay. The parametric study covered cavity diameters D = 0.5–1.0 m, embedment depths Y = 2, 4, and 10 m, and horizontal eccentricities X = 0, 1, 6, and 10 m for a strip footing of width B = 2.0 m. Quantitatively, increasing D from 0.5 m to 1.0 m at Y = 2 m reduced the ultimate bearing capacity by ≈200 kPa (≈56.7%).

1. Introduction

Shallow foundations are essential load-transfer elements in structural systems, responsible for transmitting applied loads and self-weight to the underlying soil. The effectiveness of this transfer depends on two primary criteria: preventing shear failure in the subsoil and maintaining settlements within acceptable limits. Therefore, determining the bearing capacity of the supporting soil, the maximum stress a foundation can safely impose, has long been a central focus in geotechnical the many parameters influencing the ultimate bearing capacity of shallow foundations are foundation geometry, load eccentricity, and the mechanical properties of the subsoil, particularly its shear one critical factor often overlooked in conventional design is the presence of subsurface cavities beneath or adjacent to the foundation. These voids may be naturally occurring, such as in karstic limestone formations, or anthropogenic, as in the case of tunnels, abandoned qanats, or sewer pits. Particularly in urban environments, these cavities can form close to or directly below existing structures, compromising foundation performance and stability.

With increasing urbanization and population growth worldwide, the demand for subsurface infrastructure, including transportation tunnels, utility corridors, and metro lines, has surged. Surface-level construction in densely built environments is often constrained by limited space, high costs, and potential disruptions to existing infrastructure. As a result, underground development has become an attractive and viable solution. However, such development presents several geotechnical challenges,

* Corresponding author.
E-mail addresses: vghaseminejad@gmail.com (V. Ghaseminejad).

https://doi.org/10.22080/ceas.2025.29867.1036
ISSN: 3092-7749/
How to cite this article: Garakaninezhad, A., Amiri, S., Ghomi, F. Finite Developing Inelastic Jerk Spectra for Pulse-Like Earthquakes. Civil Engineering and Applied Solutions. 2026; 2(2): 71–84. doi:10.22080/ceas.2025.29867.1036.

particularly the potential for ground deformation and surface settlement caused by excavation. These displacements can adversely affect shallow foundations located near the surface. Although modern mechanized tunneling technologies, such as Tunnel Boring Machines (TBMs), offer some control over surface settlement by regulating face pressure, excessive pressure may lead to unintended consequences such as ground heave or changes in groundwater conditions. Regardless of the tunneling method employed, both short- and long-term displacements should be accurately predicted, and proactive measures implemented to safeguard adjacent structures. This is especially crucial for shallow foundations, which are more vulnerable to ground movements due to their proximity to the surface. The presence of shallow-buried cavities beneath foundations can intensify settlement effects and introduce stress concentrations that may lead to partial or total failure. The extent of such effects depends on the cavity's size, depth, and horizontal offset relative to the foundation's centerline. Without adequate stabilization, these voids may collapse or cause unacceptable levels of deformation. Various stabilization methods have been proposed, including grouting, construction of reinforced concrete slabs, deep foundation systems such as piles, backfilling with appropriate materials, and soil reinforcement using geosynthetics. In this study, a comprehensive numerical investigation is conducted to assess the effects of subsurface cavities on the load-bearing behavior of shallow foundations in clay soils. The modeled system includes the interaction between the footing, soil, and cavity. Key parameters such as cavity size, burial depth, and eccentricity are systematically varied. The foundation is assumed to behave as a rigid strip footing. This analysis provides insight into surface deformation patterns and the influence of underground voids on foundation capacity, offering practical guidance for geotechnical engineers designing foundations in urban environments prone to subsurface anomalies.

The presence of subsurface cavities, either natural or man-made, can significantly influence the load-bearing behavior of shallow foundations. Numerous researchers have investigated this phenomenon using analytical, numerical, and experimental methods to better understand how cavity geometry, location, and soil conditions affect foundation stability. One of the earliest studies was conducted by, who employed finite element analysis to assess the stability of strip footings overlying cavities in dense silty clay, assuming elasto-plastic soil behavior. This foundational work was extended by, who examined the settlement behavior of foundations located above single cavities. Further investigations by Baus and Wang [1] analyzed the influence of tunnel geometry and position on the bearing capacity of surface foundations and validated the results through laboratory experiments. Jao and Wang [2] performed a parametric finite element analysis using the Drucker–Prager yield criterion to study concrete-lined tunnels in soft soils such as silty clay, kaolinite, and clayey sand. Their results showed that lined tunnels improve soil confinement and reduce settlement. They introduced dimensionless ratios, including tunnel depth to footing width (*D/B*) and tunnel diameter to footing width (W/B), and concluded that the effect of cavities becomes negligible when located beyond a critical depth. Additionally, lining thickness significantly improves bearing capacity and reduces deformation. Sireesh et al. [3] evaluated the use of geocell-reinforced sand mattresses over cavities in clayey soils. Their experimental study demonstrated enhanced bearing capacity and reduced settlement, along with delayed failure propagation beneath the footing.

Lee et al. [4] proposed undrained design charts for strip footings above cavities in soft clays. By adopting a parametric approach and using finite element simulations, they found that footing eccentricity, cavity rigidity, and position strongly influence the dimensionless bearing capacity factor. Soil stiffness, cavity depth, and geometric ratios were also found to affect footing performance. Asgari and Ahmadtabar Sorkhi [5] investigated the seismic performance of offshore wind turbines on monopiles in liquefiable soils under waves, winds, and earthquakes using 3D parametric models in OpenSees. Results showed that turbine responses increase with wind speed, wave height, and seismic-induced soil liquefaction. Combined loads of earthquake, wind, and waves significantly amplify the system response, highlighting the need to consider multi-hazard effects in design.

Jahangiri et al. [6] studied applying supervised machine learning to predict maximum inter-story drift in steel diagrid structures, reducing reliance on intensive simulations. Twenty-one algorithms were evaluated, with Extra Trees, Random Forest, and Bagging showing $R^2 > 0.95$. The approach provides an efficient, accurate tool for seismic vulnerability assessment of diagrid systems. Asgari et al. [7] evaluated the axial tension and compression capacities of helical piles in dense Shahriyar sand through laboratory tests. Results show that compressive and tensile capacities can reach up to six and eleven times the shaft capacity, respectively, with performance improving for multiple helices and smaller pitches. Theoretical predictions slightly underestimated or overestimated capacities depending on pile type and loading mode. Ebadi-Jamkhaneh et al. [8] evaluated the pullout performance of helical piles in dense sand reinforced with geogrid layers. Results show that geogrid significantly enhances resistance, with single-helix piles achieving up to 518% higher capacity than plain piles, and optimal performance depending on geogrid spacing. The findings highlight the synergistic effects of pile configuration and geogrid placement for reinforced foundation design. Asgari et al. [9] studied used 3D finite element analysis to assess seismic response of pile groups in sloping liquefiable soils. Results show that pile number, position, nonlinearity, and frequency content significantly affect displacements, internal forces, and acceleration, with corner piles being most sensitive. Current design codes (JRA, API) often over- or underestimate soil pressures, highlighting the need for improved analysis for pile group design. Asadoullahtabar et al. [10] investigated the collapse and dispersion potential of loess soils in Golestan, Iran, affecting infrastructure such as gas pipelines. Laboratory and field tests showed that collapsibility contributes to soil scouring, posing risks to roads and pipelines. Chemical stabilization using cement and nano-titanium proved effective, with nano-titanium offering a more environmentally sustainable solution. Bagheri et al. [11] studied and evaluated the seismic performance of two 30-story RC buildings with conventional frames (MF) and dual systems with shear walls (MFSW) on composite piled raft foundations, considering soil–structure interaction. Results show that MFSW reduces interstory drifts by up to 56%, improves soil stress distribution, and increases seismic resilience compared to MF. Hybrid pile configurations optimize foundation performance, limiting soil shear strains and highlighting SSI-induced displacement amplifications. Asgari et al. [12] investigated seismic responses of free-field, pile group, fixed-base, and shallow/deep foundation structures with varying height-to-width ratios in saturated and dry sands. 3D nonlinear finite element analyses show that soil–foundation–structure interaction (SFSI)

can either amplify or reduce structural response depending on soil stiffness and liquefaction potential. Flexible bases reduce flexural drifts and internal forces, while saturated soils increase base shear due to higher peak accelerations. Shooshpasha and Bagheri [13] studied the effect of surcharges on seismic responses of silty sands containing fines, which are prone to liquefaction and large deformations. Fully non-linear elasto-plastic dynamic analyses with coupled liquefaction triggering were conducted under two realistic earthquake events. Results show that pore pressure alone is insufficient to assess liquefaction, and deformation-based evaluation is essential for practical engineering design. Asgari et al. [14] investigated the seismic response of sands with plastic/non-plastic fines and silts under shallow foundations. Effects of soil type, foundation surcharge, liquefiable layer thickness, and earthquake parameters, including magnitude, PGA, and duration, on dynamic behavior and soil–structure interaction were analyzed. These studies highlight the importance of understanding soil–structure–earthquake interactions for improved seismic design. In summary, prior studies unanimously demonstrate that the presence of subsurface cavities can reduce the bearing capacity and increase the settlement of shallow foundations. Key influencing parameters include cavity depth, size, shape, lining condition, and relative location to the footing. The identification of a critical depth beyond which cavities have negligible influence has been a consistent finding, supporting the need for parametric and numerical evaluation in design.

Unlike many previous studies that considered single parameters or idealized conditions, this work systematically explores the combined influence of cavity diameter, embedment depth, and horizontal eccentricity on shallow strip footings in soft clay using high-order finite elements (15-node) in PLAXIS 2D. The study provides quantitative thresholds and reduction factors (e.g., reductions up to ~56% for shallow, large cavities beneath a 2.0 m footing) to assist practising engineers in preliminary risk assessment and design decisions.

2. Numerical modeling using PLAXIS software

2.1 Model geometry and material parameters

Fig. 1 is the two-dimensional model geometry used in this study, including a strip footing placed above a subsurface cavity. The model dimensions were selected to prevent any boundary effects, ensuring that the stress bulbs induced by the footing do not interfere with the model boundaries. Based on established recommendations, the horizontal and vertical extents of the model were taken as 40 m and 30 m, respectively, which are at least five times larger than the footing width. The boundary conditions were defined in accordance with standard practice for bearing capacity analysis in finite element simulations. The vertical boundary sides were constrained in the horizontal (x) direction to prevent lateral displacement, while the bottom boundary was fully fixed in both horizontal and vertical directions to maintain overall model stability. The top boundary remained free to allow vertical deformation due to loading. These settings correspond to the “standard boundary conditions” option available in PLAXIS 2D.

In the numerical modeling process, several key assumptions were considered to accurately simulate realistic conditions. To minimize the effects of rigid boundaries, the model dimensions were selected such that its width was at least 13 times and its height at least 10 times the footing width. The analyzed footing was of strip type and was modeled as a rigid body with its self-weight included. A plane strain condition was adopted, where the footing geometry was represented by plate elements, and the load was applied linearly along the plate surface. The soil behavior was simulated using the Mohr–Coulomb constitutive model. To prevent the collapse of the cavity crown under the overburden stress, cavities lined with concrete were modeled as rigid, and their self-weight was neglected. Additionally, a reference model without any cavity was first developed for comparison purposes. All models were constructed in two dimensions, and long-term (drained) conditions were assumed for different types of clay soils, with the groundwater table defined at the base of the model. The footing was assumed to rest directly on the soil surface with zero embedment depth. The bearing capacity of the footing was evaluated under ultimate conditions rather than allowable conditions, using the tangent method to determine the ultimate bearing capacity. In the modeling procedure, the geometry of the soil, cavity, and concrete lining was first generated, followed by the application of the linear load and the footing plate (Fig. 2).

Loading was applied in the form of a uniform surcharge of 800 kPa over the footing to simulate the applied stress and facilitate bearing capacity calculations. In general, PLAXIS allows loading to be applied either as force or prescribed displacement; in this validation case, force-controlled loading was used to evaluate the ultimate bearing capacity. The material parameters for the soil layers, strip footing, and cavity fill material were adopted from the reference study by Nepal and Yadav [15], and are summarized in Tables 1 to 3.

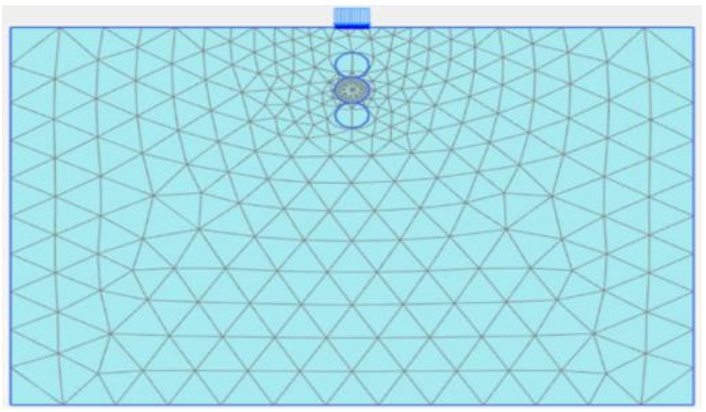

Fig. 1. Application of boundary conditions in the validation model.

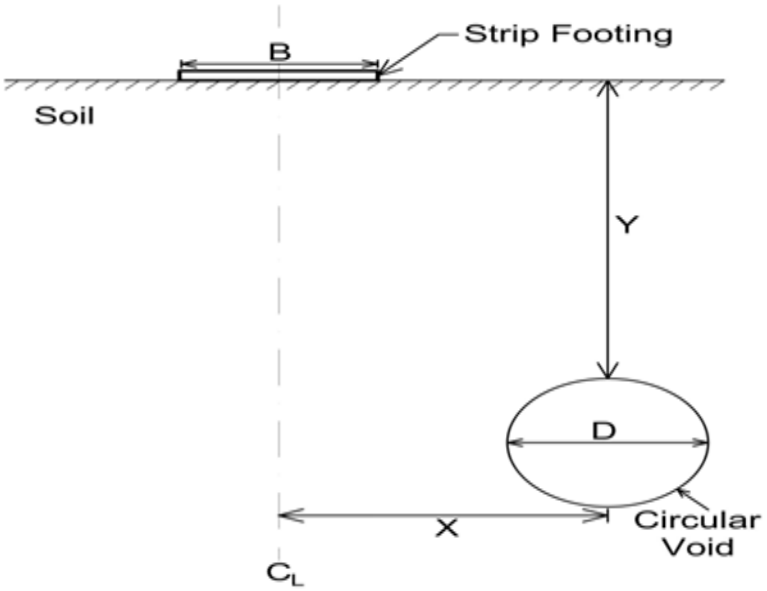

Fig. 2. Position of the cavity relative to the footing.

Table 1. Soil properties used in the study by Nepal and Yadav [15].

Geometrical Parameters	Values
Width of footing (*B*)	2 m
Width of analysis soil (*W*)	20B (40 m)
Depth of analysis soil (*D*)	15B (30 m)
Shape of void	Circular
Size of void (*D*)	2 m
Vertical position of void (*y*)	B, 2B, 3B, 4B, 5B, and 6B (from the base of the footing to the crest of the void)
Horizontal position of void (*x*)	0B, 1B, 2B, 3B, and 4B (from the center of the foundation to the center of the void)

Table 2. Geotechnical parameters in the Study by Nepal and Yadav [15].

Parameters	Values
Unit weight of soil (kN/m³)	18 (kN/m³)
Friction angle of soil, φ	34°
Young's modulus of elasticity (MN/m²)	14.6 (MN/m²)
Poisson's ratio	0.25
Dilatancy angle	4°
Cohesion	70 (kN/m²)
Failure criteria	Mohr-Coulomb
Type of material model	Drained condition

Table 3. Characteristics of the foundation investigated in Nepal and Yadav [15].

Parameters	Values
Normal stiffness (*EA*) kN/m	3×10^7
Flexural rigidity (*EI*) kN·m²/m	2×10^4
Equivalent thickness (m)	0.2
Poisson's ratio	0.1

2.2 Validation

In general, the most important part of analyzing any problem using numerical models is ensuring the. To verify the modeling, numerical analysis, and the software employed, it is necessary to utilize the results of reliable references related to the research. In this regard, a numerical study on the effect of an underground cavity on the bearing capacity of a strip footing using PLAXIS 2D software version 2022. In this section, the intended model has been simulated using PLAXIS 2D software version 2024, and its results are compared with the reference. Fig. 3 shows a comparison of the modeling results obtained from the two software versions, which demonstrates a good agreement and confirms the accuracy of the modeling performed in this study (Figs. 3 to 4).

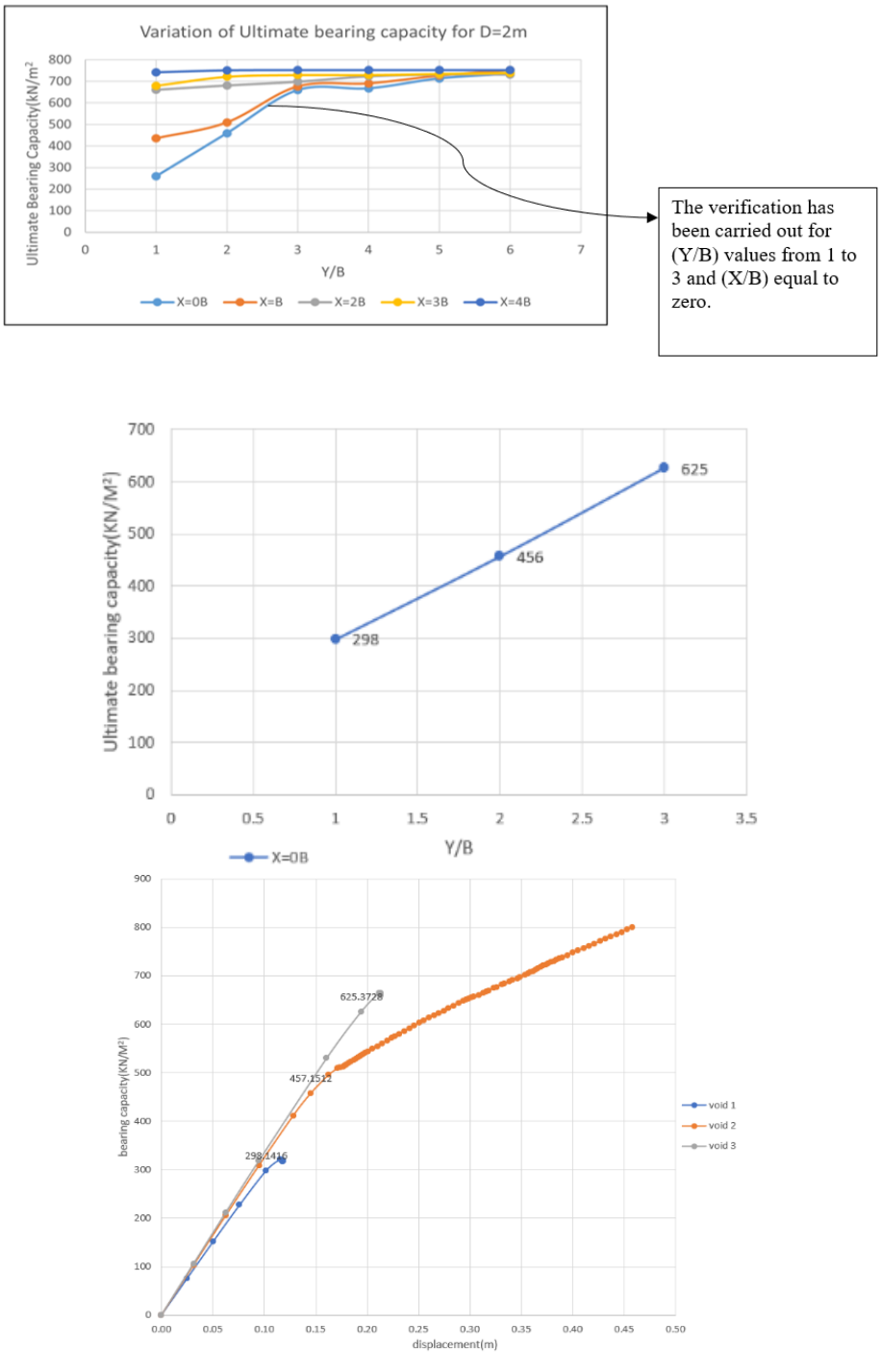

Fig. 3. Numerical results obtained using PLAXIS 2D, version 2022.

2.3 Validation results obtained through numerical simulation using PLAXIS 2D, version 2024

In this section, the results of a parametric study on the behavior of shallow foundations located above circular cavities are presented. The modeling assumptions throughout all phases of the parametric study are based on a combination of data obtained from the validated model as well as relevant textbooks and research articles. The simulations are conducted for shallow foundations placed on three types of clay: soft, medium, and stiff. The results of the modeling are compared and analyzed through a series of graphical representations.

2.3 Parametric study on the behavior of shallow foundations in the vicinity of a cavity

For the parametric investigations, the material properties listed in Table 4 are used. These properties are derived from the tables provided in the as well as the software manual used for calculating axial stiffness (*EA*) and bending stiffness (*EI*) of concrete sections in PLAXIS 2D version 2024. The calculation of both parameters, *EI* and *EA*, is performed in the third dimension, i.e., the Z-direction.

Table 4. Soil, foundation, and cavity lining properties used for numerical modeling [3].

Soil type	γ_{sat} (kN/m^3)	γ_d (kN/m^3)	C (kN/m^2)	$\varnothing$ (°)	Ψ (°)	E (kN/m^2)	R_{inter}	ν
Soft clay	16	14	10	15	0	4000	0.85	0.5
Concrete properties	E (kN/m^2)	I (m^4)	A (m^2)	EI (kN*m2)/m	EA (kN/m)	T	W (kN/m/m)	v
Concrete foundation	25*10^6	0.0104	0.5	260.4*103	12.5*106	0.5	8.27	0.2
Concrete lining of the cavity	15000	8.33*10^{-11}	0.001	1.25*10-6	15	0.001	rigid	0.1

Table 5. Abbreviations of the investigated variables.

Footing width	*B*
Cavity diameter	*D*
Cavity embedment depth	*Y*
Cavity eccentricity	*X*

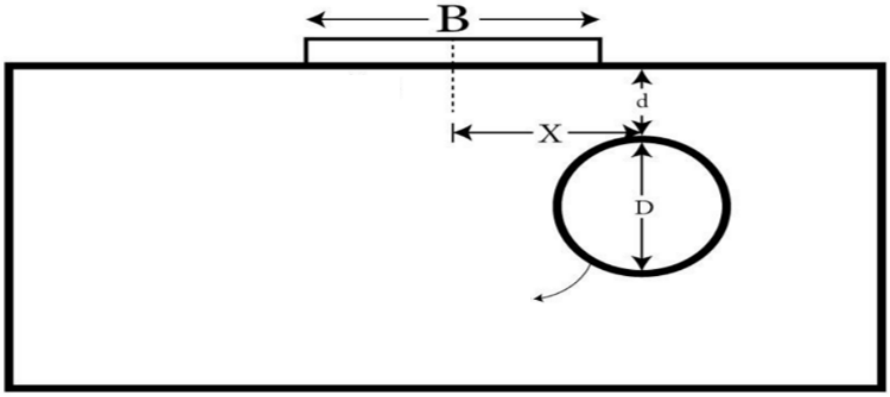

Fig. 4. Schematic representation of the components used in the numerical modeling.

3. Parametric study procedure

The parametric study in this research is organized into the following cases, based on variations in cavity diameter, embedment depth, and eccentricity, while maintaining a constant footing width of 2 meters. The soil type in all cases is varied among soft, medium, and stiff clay.

3.1. Category 1: Effect of cavity embedment depth (cavity eccentricity = 0 m*)*

In this category, the influence of cavity embedment depth on the bearing capacity of a shallow strip footing is investigated. The cavity is assumed to be located directly beneath the center of the footing (zero eccentricity), while three different diameters (0.5 m, 0.75 m, and 1.0 m) are considered. For each diameter, the cavity is placed at three different depths: 2 m, 4 m, and 10 m below the ground surface. The variations in bearing capacity due to changes in embedment depth are examined in all three soil types: soft clay, medium clay, and stiff clay.

These configurations are presented in Figs. 6 to 8, respectively.

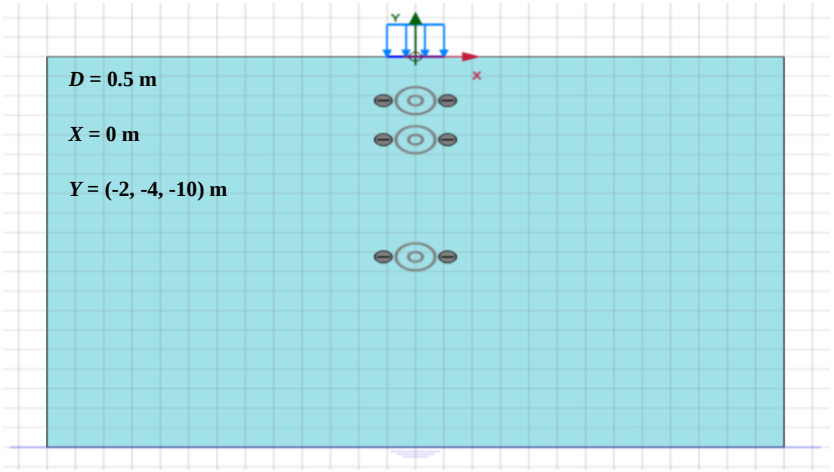

Fig. 5. Soft, medium, and stiff clay; cavity diameter: 0.5 m; cavity embedment depths: 2 m, 4 m, and 10 m.

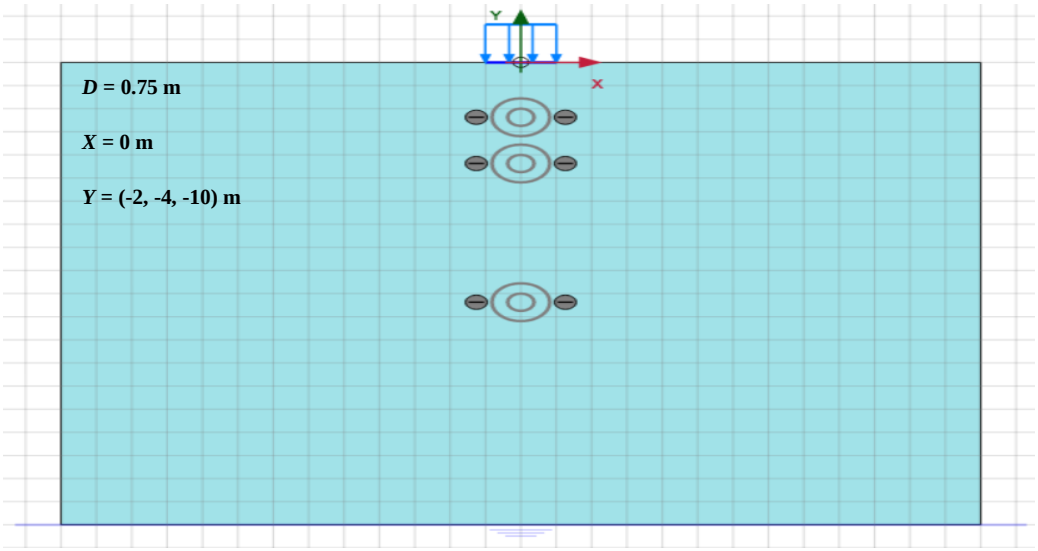

Fig. 6. Soft, medium, and stiff clay; cavity diameter: 0.75 m; cavity embedment depths: 2 m, 4 m, and 10 m.

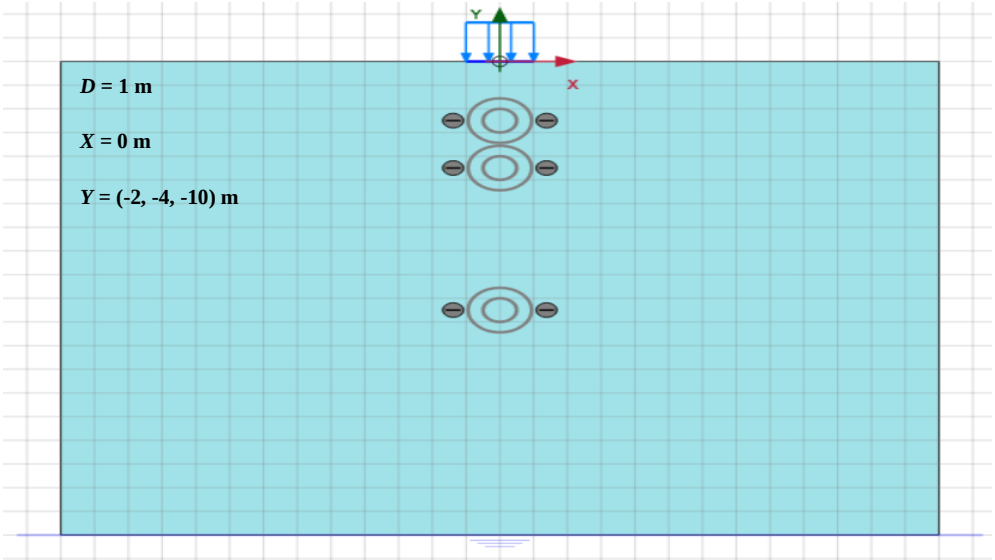

Fig. 7. Soft, medium, and stiff clay; cavity diameter: 1.0 m; cavity embedment depths: 2 m, 4 m, and 10 m.

3.2. Category 2: Effect of cavity eccentricity (fixed embedment depth = 2 m*)*

This category focuses on evaluating the effect of horizontal eccentricity of the cavity on the footing's bearing capacity. The embedment depth is kept constant at 2 meters, while the cavity diameter varies among 0.5 m, 0.75 m, and 1.0 m. For each diameter, three levels of cavity eccentricity relative to the footing center are considered: 1 m, 6 m, and 10 m. The objective is to determine the extent to which increasing horizontal distance from the footing mitigates the negative impact of the cavity.

These configurations are illustrated in Figs. 9 to 11, respectively.

In this study, the bearing capacity ratio (BCR) was defined as the ratio of the ultimate bearing capacity of a footing located above a cavity to that of an identical footing on homogeneous ground without a cavity, i.e., BCR = qu(cavity) / qu(reference). The ultimate bearing capacity (Qu) was determined from the load–settlement response obtained in PLAXIS 2D using the tangent intersection method, consistent with procedures adopted by Lee et al. [4] and Nepal and Yadav [15]. The criterion for ultimate capacity was based on the point of maximum curvature or the intersection between the initial linear (elastic) and post-yield (plastic) portions of the load–settlement curve, corresponding to the onset of general shear failure. Given that the Mohr–Coulomb model was used, the footing behavior was primarily governed by shear failure rather than settlement-controlled failure. The observed failure mechanism beneath the strip footing exhibited a general shear mode characterized by well-defined failure surfaces extending from the footing edges toward the cavity crown, in agreement with the findings of Sireesh et al. [3] and Lee et al. [4]. Therefore, the BCR values reported herein reflect reductions in the ultimate shear strength of the system due to the presence, size, and position of subsurface cavities.

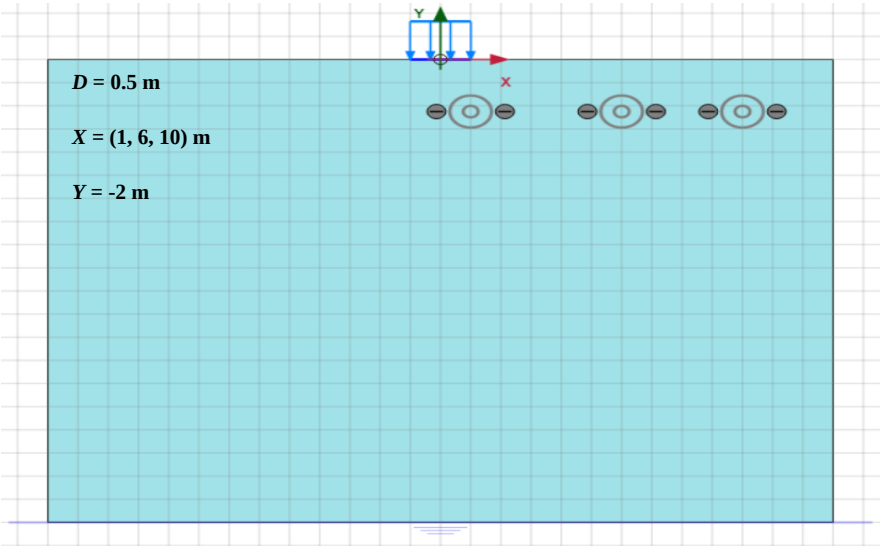

Fig. 8. Soft, medium, and stiff clay; cavity diameter: 0.5 m; cavity eccentricities: 1 m, 6 m, and 10 m; cavity embedment depth: 2 m.

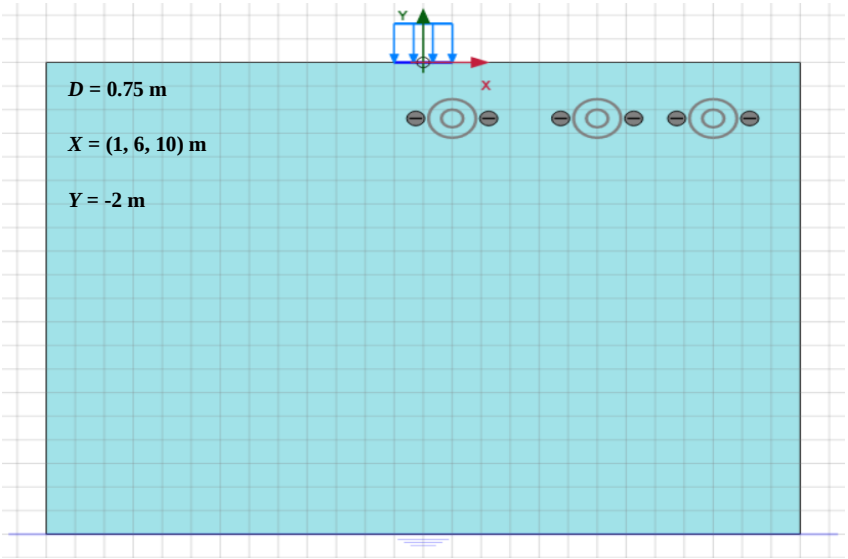

Fig. 9. Clay soil (soft, medium, hard), hole diameter 0.75 m, eccentricity 1, 6, 10 m, burial depth 2 m.

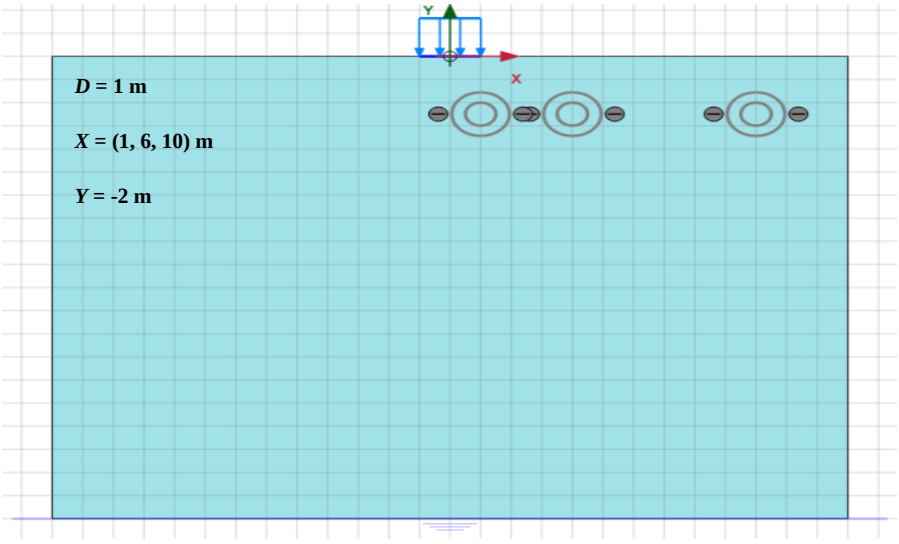

Fig. 10. Clay soil (soft, medium, hard), hole diameter 1 m, eccentricity 1, 6, 10 m, burial depth 2 m.

4. Result and discussion

4.1. Investigation of conditions (soft clay, embedment depths of 2, 4, and 10 meters, diameter of 0.5 meters) foundation specifications under isolated conditions (without cavity)

A comparison of Fig. 11 with the bearing capacity of an isolated footing in soft clay reveals that the presence of subsurface cavities with a diameter of 0.5 meters significantly influences the footing's performance. Specifically, the bearing capacity of the strip footing decreases as a function of the cavity embedment depth. The reductions in bearing capacity, relative to the isolated footing condition, are quantified as 55.79% at a depth of 2 meters, 27.37% at 4 meters, and 6.32% at 10 meters. These results indicate that increasing the embedment depth of the cavities mitigates their adverse impact, and the bearing capacity progressively converges toward that of the isolated footing, as theoretically anticipated.

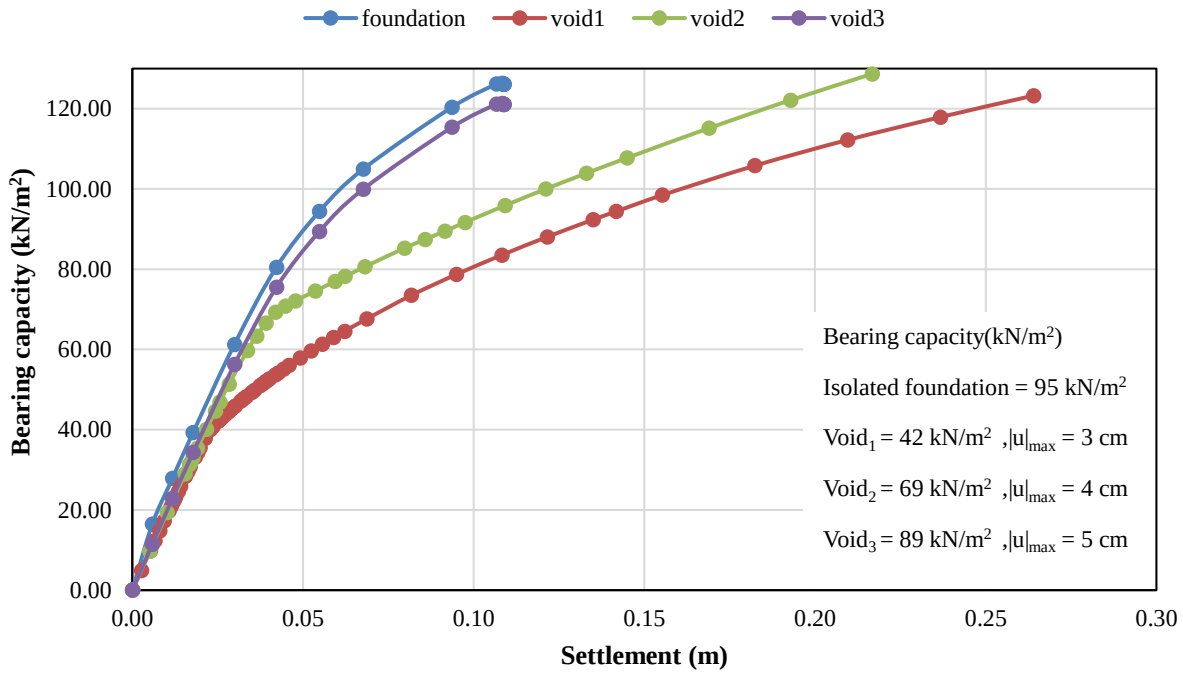

Fig. 11. Settlement graph of a strip footing with cavities of 0.5-meter diameter at various embedment depths in soft clay.

4.2. Investigation of conditions (soft clay, embedment depths of 2, 4, and 10 meters, diameter of 0.75 meters)

A comparative analysis of the figures and graphs presented in Fig. 12 with the bearing capacity of an isolated footing in soft clay indicates that the presence of cavities with a diameter of 0.75 meters beneath the footing results in a noticeable reduction in bearing capacity, depending on the embedment depth of the cavities. The observed reductions, expressed as percentages relative to the footing without cavities, are 66.32% at a depth of 2 meters, 44.21% at 4 meters, and 13.68% at 10 meters. As anticipated, the bearing capacity of the footing in the presence of cavities tends to approach that of the isolated condition as the embedment depth increases.

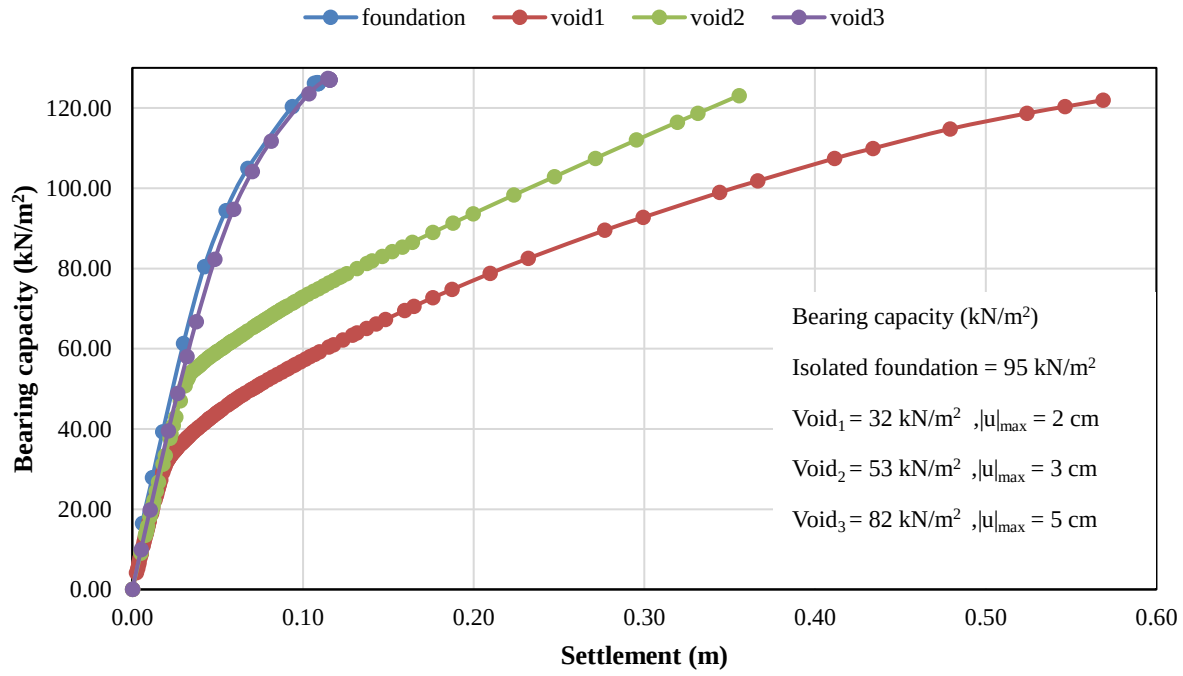

Fig. 12. Settlement graph of a strip footing with cavities of 0.75-meter diameter at various embedment depths in soft clay.

4.3. Investigation of conditions (soft clay, embedment depths of 2, 4, and 10 meters, diameter of 1 meter)

A comparison of the Fig. 13 with the bearing capacity of an isolated footing in soft clay indicates that the presence of subsurface cavities with a diameter of 1 meter significantly reduces the bearing capacity of the strip footing, depending on the embedment depth of the cavities. The reductions in bearing capacity, relative to the footing without cavities, are 72.63% at a depth of 2 meters, 56.84% at 4 meters, and 21% at 10 meters. As anticipated, increasing the embedment depth of the cavities mitigates their adverse impact, and the bearing capacity of the footing progressively approaches that of the isolated condition.

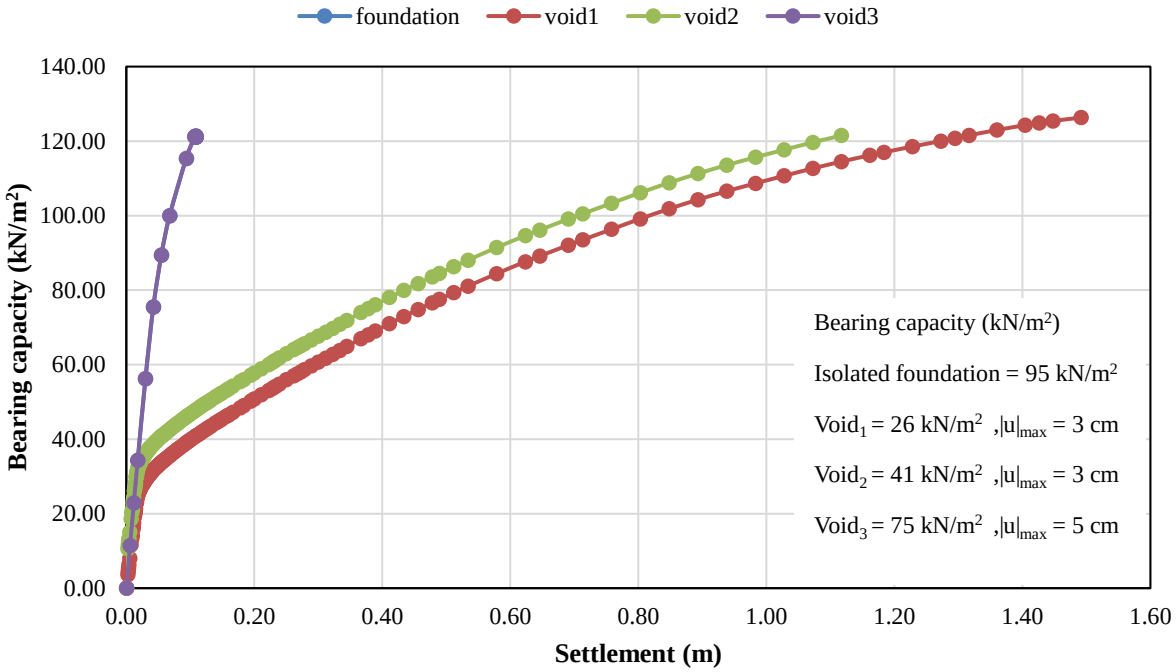

Fig. 13. Settlement graph of a strip footing with cavities of 1-meter diameter at various embedment depths in soft clay.

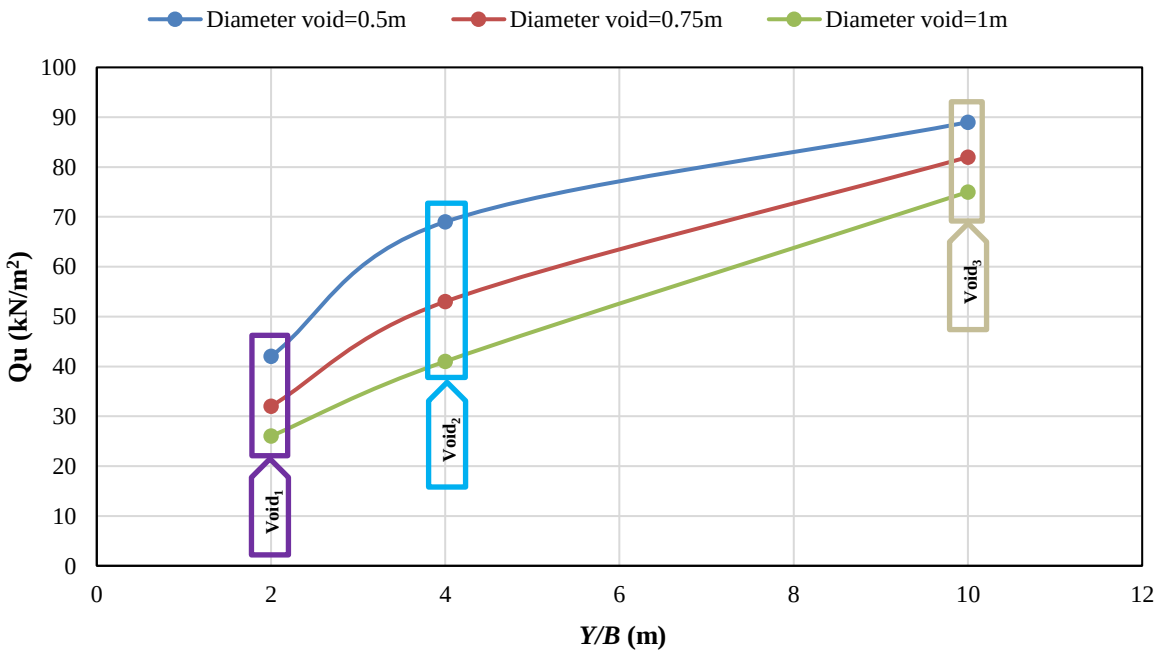

Fig. 14. Stress–depth diagram for cavities of varying diameters at different embedment depths in soft clay

A comparative analysis of the figures and graphs in Figs. 11-13 with the bearing capacity of footings containing cavities in soft clay, as illustrated in Fig. 14, indicates that the presence of subsurface cavities with diameters of 0.5, 0.75, and 1 meter beneath the footing results in a reduction of the strip footing's bearing capacity, depending on both the embedment depth and the cavity diameter. The percentage reductions, relative to the smallest cavity diameter (0.5 meters), are as follows: at an embedment depth of 2 meters, cavities with diameters of 0.75 and 1 meter cause reductions of 23.8 and 38.09%, respectively; at 4 meters, the corresponding reductions are 23.19 and 40.57%; and at 10 meters, they are 7.86 and 15.73%. Consequently, as expected, the bearing capacity of

the footing decreases progressively with increasing cavity diameter.

4.4. Investigation of conditions (soft clay, eccentricities of 1, 6, and 10 meters, diameter of 0.5 meters)

A comparison of the figures and graphs in Fig. 15 with the bearing capacity of an isolated footing in soft clay indicates that the presence of subsurface cavities with a diameter of 0.5 meters beneath the footing reduces the bearing capacity of the strip footing, depending on the cavity eccentricity. The percentage reductions relative to the footing without cavities are 49.5, 25.26, and 9.5% for cavity eccentricities of 1 meter, 6 meters, and 10 meters, respectively. As anticipated, the bearing capacity of the footing with cavities progressively approaches that of the isolated footing as the cavity eccentricity increases.

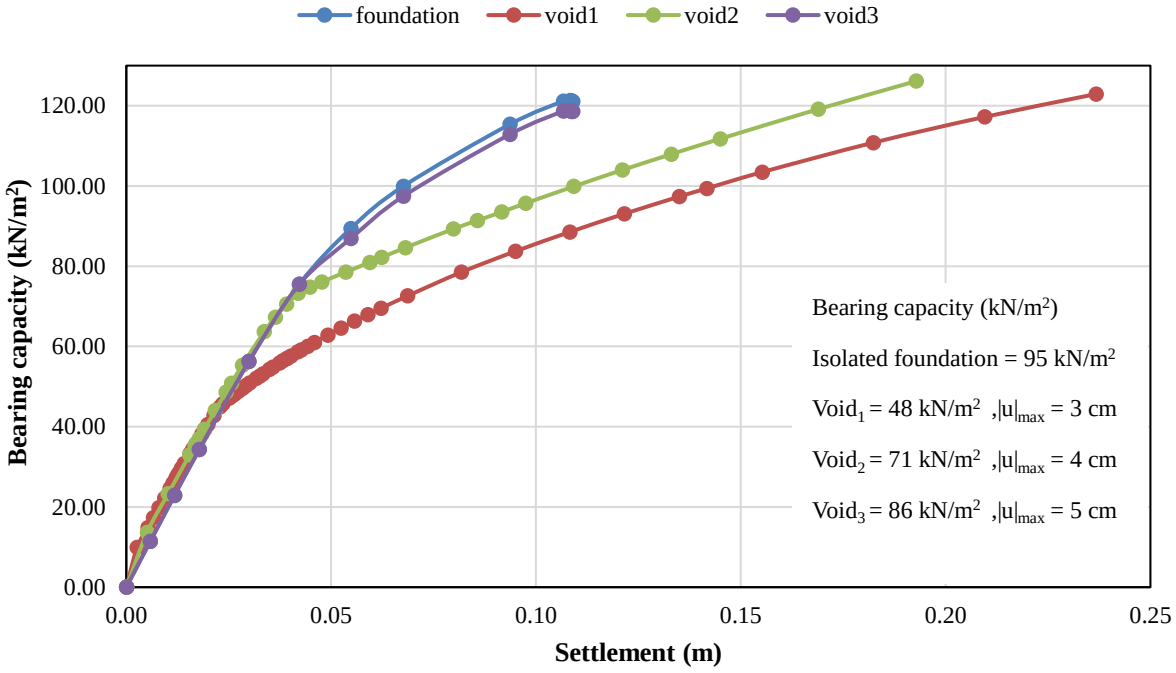

Fig. 15. Settlement graph of a strip footing with cavities of 0.5-meter diameter at various eccentricities from the footing center in soft clay.

4.5. Investigation of conditions (soft clay, eccentricities of 1, 6, and 10 meters, diameter of 0.75 meters)

A comparison of the figures and graphs in Fig. 16 with the bearing capacity of an isolated footing in soft clay indicates that the presence of subsurface cavities with a diameter of 0.75 meters beneath the footing reduces the bearing capacity of the strip footing, depending on the cavity eccentricity. The percentage reductions relative to the footing without cavities are 57.9%, 38.9%, and 11.57% for cavity eccentricities of 1 meter, 6 meters, and 10 meters, respectively. As expected, the bearing capacity of the footing with cavities progressively approaches that of the isolated footing as the cavity eccentricity increases.

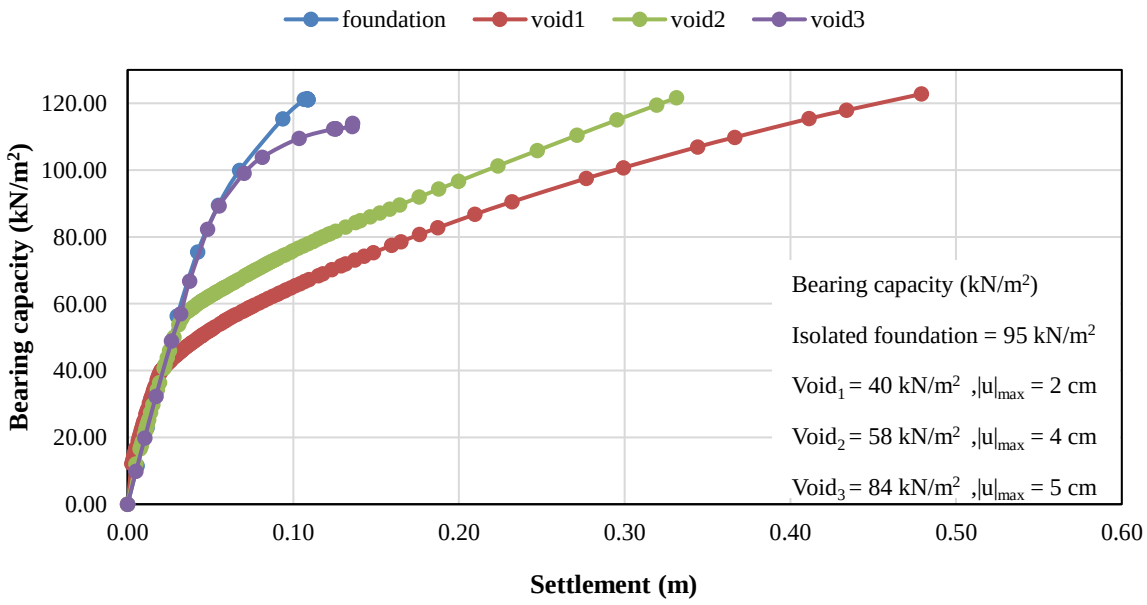

Fig. 16. Settlement graph of a strip footing with cavities of 0.75-meter diameter at various eccentricities from the footing center in soft clay.

4.6. Investigation of conditions (soft clay, eccentricities of 1, 6, and 10 meters, diameter of 1 meter)

A comparison of the figures and graphs in Fig. 17 with the bearing capacity of an isolated footing in soft clay indicates that the presence of subsurface cavities with a diameter of 1 meter beneath the footing reduces the bearing capacity of the strip footing, depending on the cavity eccentricity. The percentage reductions relative to the footing without cavities are 64.21%, 54.7%, and 16.8% for cavity eccentricities of 1 meter, 6 meters, and 10 meters, respectively. As expected, the bearing capacity of the footing with cavities progressively approaches that of the isolated footing as the cavity eccentricity increases.

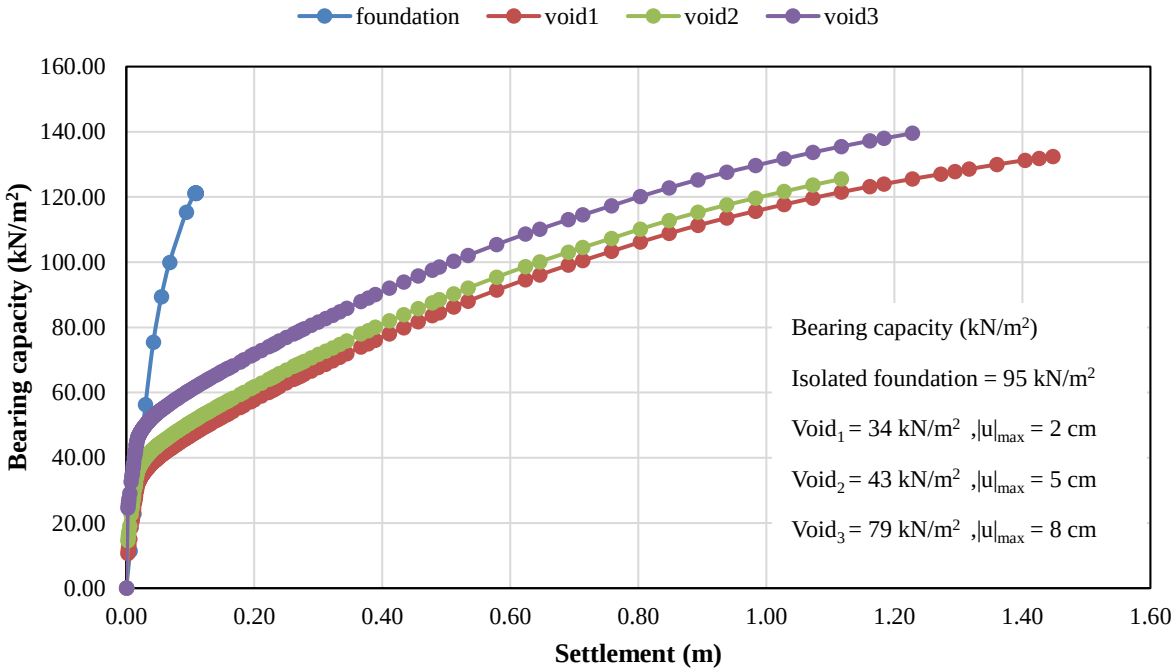

Fig. 17. Settlement graph of a strip footing with cavities of 1-meter diameter at various eccentricities from the footing center in soft clay.

A comparative analysis of the figures and graphs in Fig. 15 to 17 with the bearing capacity of footings containing cavities in soft clay, as illustrated in Fig. 18, indicates that the presence of subsurface cavities with diameters of 0.5, 0.75, and 1 meter beneath the footing leads to a reduction in the strip footing's bearing capacity, depending on both the cavity eccentricity and diameter. The percentage reductions, relative to the smallest cavity diameter (0.5 meters), are as follows: at an eccentricity of 1 meter, cavities with diameters of 0.75 and 1 meter produce reductions of 16.66 and 29.16%, respectively; at 4 meters, the reductions are 18.30 and 39.43%; and at 10 meters, they are 2.32 and 8.14%. Consequently, as expected, the bearing capacity of the footing decreases progressively with increasing cavity diameter.

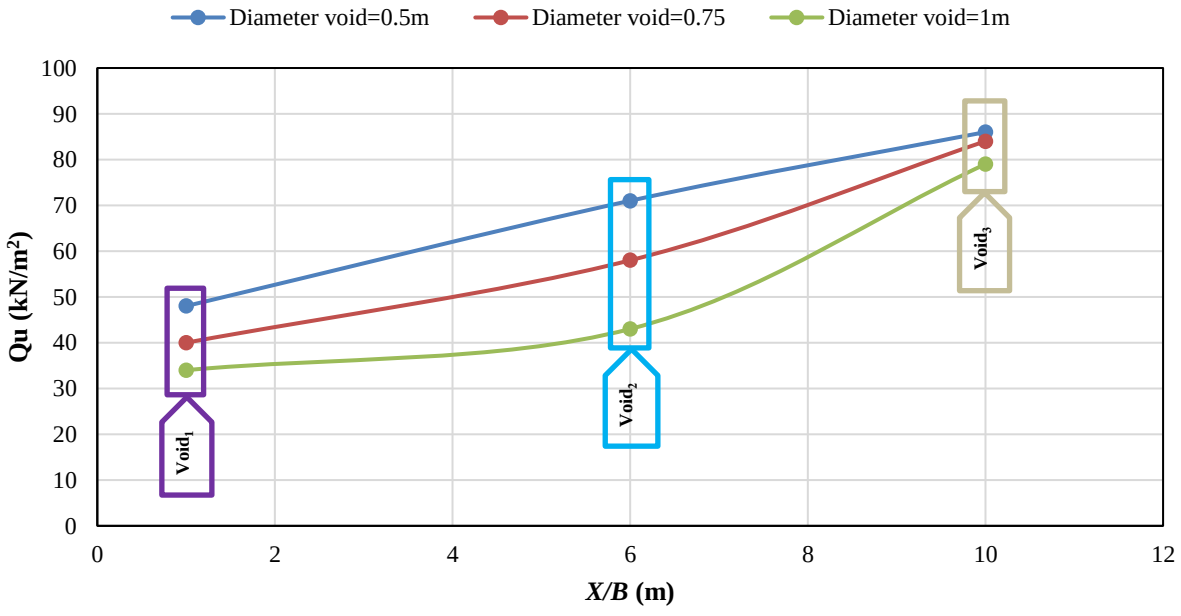

Fig. 18. Stress–eccentricity diagram for cavities of varying diameters in soft clay.

Ultimate bearing capacity was identified using the tangent intersection method, in which the extension of the initial linear slope intersects the load–settlement curve at the point of significant deviation. For curves that did not exhibit clear nonlinearity, the settlement criterion of 0.1B (10% of footing width) was adopted, as recommended in classical bearing capacity theories (Terzaghi, 1943; IS:6403–1981). This dual approach ensures consistency across all simulated cases.

5. Conclusion

This study investigates the behavior of shallow strip foundations in the presence of underground cavities within soft clay. Such cavities may exist during construction or develop later due to human or natural activities, potentially compromising part or all of the foundation's bearing capacity if located within the stress distribution zone beneath the footing. A numerical approach using PLAXIS 2D was adopted to evaluate the effects of cavity diameter, burial depth, and horizontal and vertical offsets relative to the foundation center. The soil was modeled as soft clay using the Mohr-Coulomb constitutive model.

The numerical investigation clearly demonstrates that the presence of subsurface cavities in soft clay significantly reduces the bearing capacity of strip footings. The extent of reduction is governed by cavity embedment depth and eccentricity, as well as cavity diameter. Results reveal that shallow cavities (2 m depth) exert the most detrimental effects, causing bearing capacity reductions of up to 72.63% for a cavity diameter of 1 m, whereas deeper cavities (10 m depth) mitigate adverse effects with reductions as low as 6.32%. Similarly, increasing cavity eccentricity reduces its influence, with reductions decreasing from nearly 65% at 1 m eccentricity to less than 17% at 10 m. Comparative analysis across cavity diameters confirms that larger cavities consistently induce greater reductions in bearing capacity, highlighting the combined importance of diameter and positional factors. Overall, the findings emphasize the necessity of considering both depth and eccentricity of subsurface cavities in geotechnical design. Proper assessment of these parameters is essential to ensure the safety and stability of shallow foundations in soft clay deposits.

Statements & Declarations

Author contributions

Vali Ghaseminejad: Conceptualization, Methodology, Formal analysis, Writing - original draft.

Atina Tarrah: Investigation, Data curation, Validation.

Fereshteh Ghomi: Supervision, Writing - Review & Editing.

Funding

The authors received no financial support for the research, authorship, and/or publication of this article.

Data availability

The data presented in this study will be available on interested request from the corresponding author.

Declarations

The authors declare no conflict of interest.

References

[1] Baus, R. L., Wang, M. C. Bearing Capacity of Strip Footing above Void. Journal of Geotechnical Engineering, 1983; 109: 1-14. doi:10.1061/(ASCE)0733-9410(1983)109:1(1).

[2] Jao, M., Wang, M. C. Stability of strip footings above concrete-lined soft ground tunnels. Tunnelling and Underground Space Technology, 1998; 13: 427-434. doi:10.1016/S0886-7798(98)00085-6.

[3] Sireesh, S., Sitharam, T. G., Dash, S. K. Bearing capacity of circular footing on geocell–sand mattress overlying clay bed with void. Geotextiles and Geomembranes, 2009; 27: 89-98. doi:10.1016/j.geotexmem.2008.09.005.

[4] Lee, J. K., Jeong, S., Ko, J. Undrained stability of surface strip footings above voids. Computers and Geotechnics, 2014; 62: 128-135. doi:10.1016/j.compgeo.2014.07.009.

[5] Asgari, A., Ahmadtabar Sorkhi, S. F. Wind turbine performance under multi-hazard loads: Wave, wind, and earthquake effects on liquefiable soil. Results in Engineering, 2025; 26: 104647. doi:10.1016/j.rineng.2025.104647.

[6] Jahangiri, V., Akbarzadeh, M. R., Shahamat, S. A., Asgari, A., Naeim, B., Ranjbar, F. Machine learning-based prediction of seismic response of steel diagrid systems. Structures, 2025; 80: 109791. doi:10.1016/j.istruc.2025.109791.

[7] Asgari, A., Arjomand, M. A., Bagheri, M., Ebadi-Jamkhaneh, M., Mostafaei, Y. Assessment of Experimental Data and Analytical Method of Helical Pile Capacity Under Tension and Compressive Loading in Dense Sand. Buildings, 2025; 15: 2683.

[8] Ebadi-Jamkhaneh, M., Arjomand, M. A., Bagheri, M., Asgari, A., Nouhi Hefzabad, P., Salahi, S., Mostafaei, Y. Experimental Study on the Pullout Behavior of Helical Piles in Geogrid-Reinforced Dense Shahriyar Sand. Buildings, 2025; 15: 2963.

[9] Asgari, A., Ranjbar, F., Bagheri, M. Seismic resilience of pile groups to lateral spreading in liquefiable soils: 3D parallel finite element modeling. Structures, 2025; 74: 108578. doi:10.1016/j.istruc.2025.108578.

[10] Asadoullahtabar, S. R., Asgari, A., Mohammad Rezapour Tabari, M. Assessment, identifying, and presenting a plan for the stabilization of loessic soils exposed to scouring in the path of gas pipelines, case study: Maraveh-Tappeh city. Engineering Geology, 2024; 342: 107747. doi:10.1016/j.enggeo.2024.107747.

[11] Bagheri, M., Ranjbar Malidarreh, N., Ghaseminejad, V., Asgari, A. Seismic resilience assessment of RC superstructures on long–short combined piled raft foundations: 3D SSI modeling with pounding effects. Structures, 2025; 81: 110176. doi:10.1016/j.istruc.2025.110176.

[12] Asgari, A., Bagheri, M., Hadizadeh, M. Advanced seismic analysis of soil-foundation-structure interaction for shallow and pile foundations in saturated and dry deposits: Insights from 3D parallel finite element modeling. Structures, 2024; 69: 107503. doi:10.1016/j.istruc.2024.107503.

[13] Shooshpasha, I., Bagheri, M. The effects of surcharge on liquefaction resistance of silty sand. Arabian Journal of Geosciences, 2014; 7: 1029-1035. doi:10.1007/s12517-012-0737-9.

[14] Asgari, A. L. I., Golshani, A., Bagheri, M. Numerical evaluation of seismic response of shallow foundation on loose silt and silty sand. Journal of Earth System Science, 2014; 123: 365-379. doi:10.1007/s12040-013-0393-9.

[15] Nepal, B., Yadav, S. K. Numerical Study of Bearing Capacity under Strip Footing having Underground Void. In: Proceedings of 14th IOE Graduate Conference; 2023 Nov 29-Dec 1; lalitpur, Nepal. p. 727-731.